

RARAF – Table of Contents

RARAF Staff and Picture.....	66
Research Using RARAF	67
Development of Facilities	70
Accelerator Utilization and Operation	73
Training.....	74
Personnel.....	74
Recent Publications of Work Performed at RARAF (2003-2004).....	74

RARAF PROFESSIONAL STAFF

- David J. Brenner**, Ph.D., D.Sc. – RARAF Director
Stephen A. Marino, M.S. – RARAF Manager
Gerhard Randers-Pehrson, Ph.D. – RARAF Associate Director, Chief Physicist
Charles R. Geard, Ph.D. – CRR Associate Director, Senior Biologist
Alan Bigelow, Ph.D. – Associate Research Scientist
Brian Ponnaiya, Ph.D. – Associate Research Scientist
Guy Y. Garty, Ph.D. – Staff Associate
Gregory Ross, Ph.D. – Programmer Analyst
Stephen Mitchell, Ph.D. – Post-Doctoral Research Scientist
Giuseppe Schettino, Ph.D. – Post-Doctoral Research Scientist
Gloria Jenkins-Baker, B.A. – Biology Technician



RARAF Staff (l-r): David Brenner, Brian Ponnaiya, Gloria Jenkins-Baker, Charles Geard, Stephen Mitchell, Guy Garty, Gerhard Randers-Pehrson, Alan Bigelow, Giuseppe Schettino, Gregory Ross and Stephen Marino.

The Radiological Research Accelerator Facility

AN NIH-SUPPORTED RESOURCE CENTER – WWW.RARAF.ORG

Director: David J. Brenner, Ph.D., D.Sc.

Manager: Stephen A. Marino, M.S.

Chief Physicist: Gerhard Randers-Pehrson, Ph.D.

This is a major year for RARAF. Our Van de Graaff accelerator, which is 55 years old and has provided us with charged particle beams for over 38 years, will be decommissioned this May. We will install a new Singletron from High Voltage Engineering (HVE) that should provide us with increased voltage, stability and beam current.

Among the major accomplishments this year:

- The first microbeam irradiations using the new microbeam facility (Microbeam II);
- Construction of a successful quadrupole triplet, producing a helium ion beam spot 3.5 μm in diameter;
- Construction of the stand-alone microbeam vacuum system and installation and testing of the quadrupole magnets.

Research Using RARAF

For several years, the focus of most of the biology experiments at RARAF has been the “bystander” effect, in which cells that are not irradiated show a response to radiation when in close contact with or even only in the presence of irradiated cells. Several experiments examining this effect were continued this year and new ones initiated, observing a variety of endpoints to determine the size of the effect and the mechanism(s) by which it is transmitted. Evidence has been obtained for both direct gap junction communication through cell membrane contact and indirect, long-range communication through media transfer. In some experiments, the unirradiated cells can be identified due to differential staining and scored directly, in other experiments unirradiated cells are physically separated from the irradiated cells during irradiation. Both the microbeam and the track segment facilities continue to be utilized in various investigations of this phenomenon. The single-particle microbeam facility provides precise control of the number and location of particles so that irradiated and bystander cells may be distinguished but is somewhat limited in the number of cells that can be irradiated. The track segment facility provides broad beam irradiation that provides a random pattern of charged particles but allows large numbers of cells to be irradiated and multiple users in a single day.

In Table I are listed the experiments performed at RARAF from November 1, 2003 through October 31, 2004 and the number of days each was run in this period. Use of the accelerator for experiments was 50% of the normal available time, 50% higher than last year and the highest we have attained at Nevis Labs. In addition, for the first time in over a decade outside users accounted for half the experiment time. Sixteen different experiments were run during this period, about the same as the average for 1997–2003.

Seven experiments were undertaken by members of the CRR, supported by grants from the National Institutes of Health (NIH) and the Department of Energy (DOE). Nine experiments were performed by outside users, supported by grants and awards from the NIH, the National Aeronautics and Space Administration (NASA), the National Science Foundation (NSF), and the Ministry of Education, Science, Sports and Culture of Japan. Brief descriptions of these experiments follow.

Eric Hall and Stephen Mitchell of the Center for Radiological Research (CRR) continued investigations involving the oncogenic neoplastic transformation of mouse C3H 10T $\frac{1}{2}$ cells (Exp. 73). Using the microbeam facility, 10% of the cells were irradiated through the nucleus with 2 to 12 helium ions. Cells were plated at densities of approximately 200 and 2000 per dish to try to observe the relative contribution of cell-cell communication to the bystander effect. Cell killing and transformation were greater for the cells plated at the higher density relative to those plated at the lower density. The results imply that gap junction communication has a greater role in the bystander effect than media transfer. In another aspect of the study, a novel radiation apparatus where irradiated and non-irradiated cells were grown in close proximity was used to investigate the relationship between the bystander effect and adaptive response in C3H 10T $\frac{1}{2}$ cells. Special “strip” track segment dishes were made by cutting the Mylar surface on the bottom of special cell dishes into many equal strips and removing alternate strips. The remaining Mylar strips are sufficiently thick to stop the incident ions, so that cells plated on these surfaces are not irradiated. These dishes were placed inside standard track segment dishes that have a complete Mylar surface 6 μm thick, through which the ions readily pass. Cells are plated on the combined surface. When the cells were left *in situ* for 24 h for the non-hit cells to co-culture with cells irradiated with 5 Gy of α -particles using the track segment facility, a significant increase in both cell killing and oncogenic transformation frequency was observed. If these cells were treated with 2 cGy of x-rays 5 h prior to co-culture with irradiated cells, approximately 95% of the bystander effect was canceled out. A 2.5-fold decrease in the oncogenic transformation frequency was also observed. To investigate whether mouse embryo fibroblast cells haplo-insufficient for one or more of a number of genes of known importance, namely *ATM*, *BRCA1* and *RAD9*, are radiosensitive to cell lethality and/or oncogenic transformation, cells that are heterozygous for these genes were irradiated on the track segment facility. To date no difference has been seen for survival, whereas cells haplo-insufficient for both *ATM* and *RAD9* are signifi-

Table I.
Experiments Run at RARAF, Nov. 1, 2003–Oct. 31, 2004

Exp. No.	Experimenter	Institution	Exp. Type	Title of Experiment	No. Days Run
73	S. Mitchell, E.J. Hall	CRR	Biology	Neoplastic transformation of mouse cells by α -particles	6.9
82	R. Eliassi, (G. Garty)	UCLA	Physics	1. Detection of explosives	9.8
89	R. H. Maurer, et al.	Johns Hopkins University	Physics	2. Calibration of a portable real-time neutron spectrometry system	0.6
92	S. Amundson	NIH	Biology	Functional genomics of cellular response to high-LET radiation	5.0
94	B. Ponnaiya, C.R. Geard	CRR	Biology	Single cell responses in hit and bystander cells: single-cell RT-PCR and protein immunofluorescence	8.3
103	G. Jenkins, C.R. Geard	CRR	Biology	Damage induction and characterization in known hit versus non-hit human cells	9.6
106	B. Ponnaiya, C.R. Geard	CRR	Biology	Track segment alpha-particles, cell co-cultures and the bystander effect	2.3
110	H. Zhou, T.K. Hei	CRR	Biology	Identification of molecular signals of alpha-particle-induced bystander mutagenesis	13.2
113	A. Miller	AFRRI	Biology	Role of alpha-particle radiation in depleted uranium-induced cellular effects	1.0
118	R. Kolesnick, G. Perez	MSKCC; Mass. General Hosp.	Biology	Characterization of the radiosensitive target for cell death in mouse oocytes	3.5
121	A. Zhu, H. Lieberman	CRR	Biology	The bystander effect in mouse embryo stem cells with mutant <i>Mrad9</i> gene	14.6
122	K. Kosakowski	SSG Precision Optics, Inc.	Physics	Strength of epoxy joints after neutron irradiation	1.3
123	E. Aprile	CU Astrophysics	Physics	Calibration of a liquid xenon detector	22.5
125	M. Suzuki (H. Zhou)	Ntl. Inst. of Radiological Science, Japan	Biology	Chromatid fragment induction detected with the PCR technique by cytoplasmic irradiation in normal human bronchial cells	16.8
126	O. Sedelnikova (L. Smilenov)	NIH	Biology	γ -H2AX foci formation in directly irradiated and bystander cells	3.5
129	W. Morgan (S. Mitchell)	University of Maryland	Biology	Investigation of the bystander effect	6.1

Note: Names in parentheses are CRR members who collaborated with outside experimenters.

cantly more prone to transformation than wild-type cells.

Development of a method to detect explosives in baggage (Exp. 82) was resumed this year. Ravash Eliassi, an undergraduate student at UCLA, in collaboration with Guy Garty and under the guidance of Gerhard Randers-Pehrson, both of the CRR, made measurements of neutron spectra and yield from the $\text{Be}^9(p,n)$ reaction using a very thin beryllium target. The detection system is based on resonant scattering of 0.43 MeV neutrons by nitrogen and oxygen. Measurements were made for several combinations of reaction angle and incident proton energy that produce 0.43 MeV neutrons to determine parameters producing the highest yield and the spectrum that contains the highest percentage of neutrons of the desired energy.

Richard Maurer, David Roth and James Kinnison of Johns Hopkins University performed an irradiation (Exp. 89) with neutrons of a pair of charged-coupled devices (CCDs) to be used to send video signals from the NASA New Hori-

zons probe that will travel past Pluto to the outer asteroid belt. Since the probe will spend much of its life too far away to use solar panels, there will be a radioisotope thermoelectric generator (RTG) on board that uses the radioactive decay of plutonium to produce electricity. The potential effect of neutrons emitted by the plutonium on the resolution of the CCDs was determined. A neutron energy of 2.1 MeV was used because it is near the average energy of the neutrons produced by the fission of plutonium.

Sally Amundson, now a member of the CRR, is conducting two types of experiments concerning the radiation-induced gene expression profiles in human cell lines using cDNA microarray hybridization and other methods (Exp. 92). The first involves track segment irradiation for comparison of gene expression responses to direct and bystander irradiation. In these experiments, gene expression at 4 and 24 hours post treatment are compared. Early experiments have worked well and they are now being repeated to establish reproducibility and to obtain sufficient data to begin informatic analysis. The second type of irradiation involves use of the microbeam to irradiate either

cell nuclei or cytoplasm. These experiments require optimization and validation of cDNA amplification techniques to produce sufficient material for microarray hybridization from the small number of cells irradiated. Initial results indicate the system is robust and accurate. RNA from single microbeam dishes has been isolated successfully and early amplification and hybridization results are highly encouraging. Gene expression profiles have been obtained from both nuclear and cytoplasmic irradiation at 4 and 24 hours after treatment. As in the case of the track-segment bystander studies, these experiments must still be repeated to obtain reproducible data that can be analyzed to reveal gene expression trends.

Two studies investigating the bystander effect were continued by Brian Ponnaiya and Charles Geard of the CRR. In one study (Exp. 94), levels of p21 production were measured in individual normal human fibroblasts using immunofluo-

rescent staining. This procedure permits observation of the variation in response of individual cells to radiation instead of just the average response of a large number of cells. From 1 to 100% of the cell nuclei were irradiated with helium ions using the microbeam facility. The second investigation uses the track segment facility for broad-beam charged particle irradiations of human fibroblasts and epithelial cells immortalized with telomerase (Exp. 106). Special cell dishes are made from stainless steel rings with thin Mylar windows glued on both sides onto which cells are plated, eliminating any possibility of cell-cell contact between cells on opposing surfaces. The dish volume is filled with medium. Cells on one surface are irradiated with ^4He ions; cells on the opposite surface are unirradiated because the particles stop in the medium before reaching them. They have used this novel co-culturing protocol previously to demonstrate bystander responses observed by the induction of micronuclei and chromosomal aberrations in non-irradiated normal human fibroblasts following irradiation with helium ions using the track segment facility. These studies have since been expanded to include analyses of cellular signaling pathways in both irradiated and bystander cells at both the protein and mRNA levels. Cells were observed *in situ* after irradiation with doses from 0.05 to 1.6 Gy of 125 keV/ μm ^4He ions or 0.01 to 0.10 Gy of 12 keV/ μm protons. The proteins examined by immunofluorescence techniques included p21/WAF1 and members of the MAP kinase signaling pathway, i.e., ERK1/2, p38 and pJNK, whose phosphorylation status has been shown to be altered in both irradiated and bystander cells. Levels of mRNA from early response genes, including *c-fos*, *c-jun*, *junB* and *p21/WAF1* were also assayed using RT-PCR protocols.

Charles Geard and Gloria Jenkins of the CRR continued their studies of the bystander effect in several cell lines using the microbeam facility (Exp. 103). Normal human fibroblasts and human mammary epithelial cells were irradiated with helium ions, targeting 1%, 10% and 100% of the cell nuclei. Endpoints for various experiments included micronucleus production in S phase, production of p21, p53 and H2AX in the fibroblasts and production of H2AX in the mammary cells. In some of the experiments the bystander cells were stained with a dye different than the irradiated cells so the two could be distinguished.

Hongning Zhou and Tom Hei of the CRR continued to use the single-particle microbeam facility to try to identify the signaling transduction pathways involved in radiation-induced bystander mutagenesis (Exp. 110). Functional deficiency cell lines or cells treated with inhibitors are irradiated using the microbeam facility. A fraction of the cells is irradiated with alpha-particles. The cells are kept *in situ* for 2, 6, 24 or 48 hours after irradiation, thereby increasing the number of cells and the time for interaction. In addition, some experiments have been performed using the track segment facility using the "strip" dishes described for Experiment 73. The mRNA extracted from the cells is analyzed using microarrays. Preliminary data show some changes in gene expression in the bystander cells.

The Department of Defense is interested in the biological effects of depleted uranium (DU), especially after its signifi-

cant relevance to the recent wars in the Middle East. The primary focus has been the chemical effects of DU on human cells. Alexandra Miller of the Armed Forces Radiobiological Research Institute (AFRRI) continued a study of neoplastic transformation of immortalized human osteoblast cells by helium ions (Exp. 113). Graded doses of helium ions were delivered using the track segment facility to try to determine the contribution to cell transformation of the alpha-particles emitted by the DU.

Richard Kolesnick of the Memorial Sloan Kettering Cancer Center (MSKCC) and Gloria Perez of Massachusetts General Hospital continued their efforts to try to determine whether the radiosensitive target for mouse oocyte killing (Exp. 118) is the DNA, the plasma membrane or the cytoplasm. Understanding what the target is would help in the development of protective therapies to prevent the side effects of radiotherapy on female germ cells. For these experiments they have selected the mouse strain C57BL/6 because oocytes from these mice show low rates of spontaneous apoptosis. Mature and immature oocytes are irradiated in the nucleus, the cytoplasm or the cell membrane using the microbeam facility. Because the oocytes are spherical with a uniform diameter of about 80 μm , they are irradiated with protons because the range of the helium ions is insufficient to penetrate much more than half way through the cells.

Howard Lieberman and Aiping Zhu of the CRR have completed experiments investigating the bystander effect in mouse embryonic stem cells with a mutation in the *Mrad9* gene (Exp. 121), which promotes radiation resistance and helps regulate the cell cycle and apoptosis. Cells plated on the special "strip" dishes were irradiated with 1 to 10 Gy of helium ions using the track segment facility and observed for cell survival, micronucleus production and apoptosis. Cells with the mutated gene show an enhanced bystander effect. The study was expanded to observe the survival of directly irradiated cells for LETs in the range 12 to 180 keV/ μm . The cells with the mutated gene had significantly lower survival than normal cells for 12 keV/ μm protons but there was little or no difference for 125 keV/ μm helium ions, and these cohorts were growth phase dependent.

Irradiations with 2.1 MeV neutrons were performed for Kris Kosakowski of SSG Precision Optics, Inc. (Exp. 122). His company is sending optical lenses on the New Horizons space probe mentioned above for Exp. 89. Part of the lens mounts consist of blocks of Invar epoxied to silicon carbide. The lenses had to be tested for degradation of their optical properties by neutron exposure from the RTG power supply and the lens mounts were tested for changes in the bonding strength of the epoxy.

A group led by Elena Aprile of the Astrophysics section of Columbia University, in collaboration with researchers from Yale and Brown Universities, is calibrating a liquid xenon proportional counter (Exp. 123) to be used to detect WIMPs (weakly interacting massive particles). These are heavy neutral particles that only interact weakly with matter and may be the "dark matter" that will make up the "missing" mass required to "close" the universe, i.e. eventually cause the present expansion to reverse and implode. Neutrons scattered at a fixed angle by the xenon are detected in

coincidence with pulses produced by the neutrons in the xenon detector. Since the initial neutron energy is known, the energy imparted to the xenon nucleus can be calculated. This energy divided by the height of the xenon detector pulse provides the calibration of the detector.

Masao Suzuki of the National Institute of Radiological Science, Japan, in collaboration with Hongning Zhou of the CRR, continued his efforts to determine whether alpha-particle irradiation can induce a bystander response in primary human bronchial epithelial (NHBE) cells (Exp. 125), extending the study to bystanders of cytoplasmic irradiation. Either all or ten percent of the cells were irradiated in the cytoplasm with helium ions using the microbeam facility. The cells were then accumulated in the G2 phase of the cell cycle and the process of premature chromosome condensation (G2PCC) was used to observe chromatin aberrations. Preliminary data show cytoplasmic alpha-particle irradiation can induce a bystander effect. However, more irradiated cells as well as non-irradiated bystander cells are needed to further confirm the results.

The occurrence of non-targeted effects calls into question the use of simple linear extrapolations of cancer risk to low doses from data taken at higher doses. Olga Sedelnikova of the NIH, in collaboration with Lubomir Smilenov of the CRR, is investigating a model for bystander effects that would be potentially applicable to radiation risk estimation (Exp. 126). They are evaluating the lesions that are introduced into DNA by alpha-particles and the resulting non-targeted bystander effect. These lesions, and particularly the most dangerous – double strand breaks (DSB), can be revealed by phosphorylation of the histone H2AX. Primary WI38 human epithelial cells stained with Hoechst dye that is visible to the microbeam imaging system are mixed with others stained with cyto-orange (bystanders) that are not visible. The cells dyed with the Hoechst stain are irradiated with graded numbers of alpha-particles. The numbers of DSB in directly irradiated cells and in non-hit cells in close proximity to an irradiated cell are estimated by phosphorylation of the histone H2AX. The results from these experiments as well as from experiments from other labs will be used to make an overall best assessment of the public health significance of bystander-mediated responses.

William Morgan of the University of Maryland, in collaboration with Stephen Mitchell of the CRR, performed an investigation of the bystander effect (Exp. 129) using the GM10115 cell line which does not show gap junction communication. Cells were irradiated with 2 to 12 helium ions using the microbeam facility or were plated on the “strip” dishes described in Exp. 73 and given a dose of 5 Gy of helium ions using the track segment facility. No difference was seen for cell killing, emphasizing the importance of gap junctions in mediating the bystander response.

Development of Facilities

Our development effort has somewhat decreased this year from last but is still very high. We have added another person to the development team: Giuseppe Schettino, who developed the x-ray microbeam for the Gray Cancer Institute.

Development continued or was initiated on the microbeam facilities and a number of extensions of their capabilities:

- Development of focused accelerator microbeams
- Source-based microbeam
- Focused x-ray microbeam
- Precision z-motion stage
- Laser ion source
- Secondary emission ion microscope (SEIM) for viewing focused beam spots
- Non-scattering particle detector
- Advanced imaging systems
- New accelerator

Development of focused accelerator microbeams

A quadruplet lens with titanium-coated rods was mounted in the alignment tube for the double lens system and placed in the beam line for the new microbeam facility. It focused the beam to less than a 7 μm diameter. Measurements made of the voltages required to obtain various beam spot geometries when all and only some of the lens elements were used provided data for our consultant at the University of Louisiana, Alexander Dymnikov, to calculate parameters for the double quadrupole triplet lens assembly that will be used to focus the ion beam to a diameter of 0.5 μm .

The first quadrupole triplet based on these calculations has been constructed, placed in a separate alignment tube and inserted in the beam line in place of the quadruplet lens. This triplet lens has produced a beam spot for helium ions 3.5 μm in diameter. It required very little voltage conditioning, produced an acceptable beam in less than a week of adjustments and has been used for microbeam irradiations for several months. The second quadrupole triplet is under construction in our shop and will be inserted for testing in place of the present one, once it is completed. When the voltages on this second lens have been adjusted to produce the smallest beam spot attainable, the two lenses will be mounted in a single tube for testing of the compound lens system that will produce a sub-micron beam spot.

Source-based microbeam

A stand-alone microbeam (SAM) has been designed based on a small, relatively low activity radioactive alpha-particle emitter (5 mCi ^{210}Po) plated on the tip of a 1-mm diameter wire. Alpha-particles emitted from the source will be focused into a spot 10 μm in diameter using a compound quadrupole lens made from commercially available permanent magnets, since only a single type and energy of particle will be focused. The pair of quadrupole triplets is similar to the one designed for the sub-micron microbeam, the only difference being that it uses magnetic lenses, rather than electrostatic lenses. A small stepping motor rotating a disc with holes will be placed just above the source to chop the beam, enabling single particle irradiations. The end station for the original microbeam will be used to perform microbeam irradiations. The SAM will replace the accelerator-based system in our original microbeam laboratory and can be used during the period when the Van de Graaff is being removed and the Singletron installed.

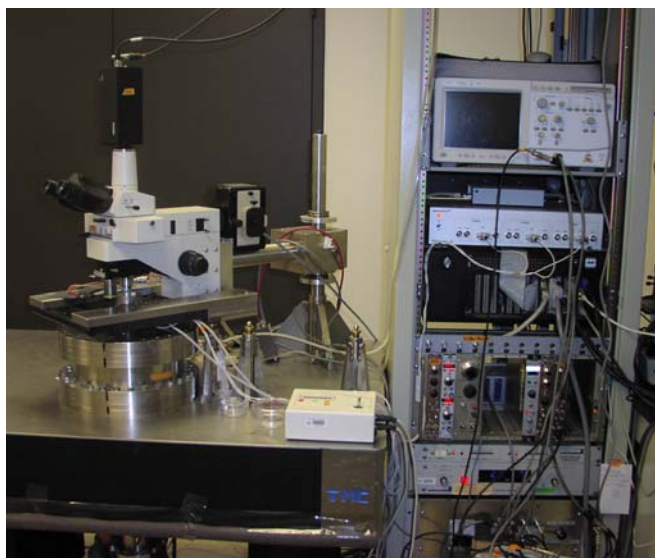


Fig. 1 The new microbeam irradiation station (Microbeam II). On the right is a rack containing most of the electronics for the camera, moving the stage and data acquisition. The Mad City stage is in place on the microscope. The pivot for moving the microscope between the on-line and off-line positions is in the center of the picture.

The magnets have been received and mounted in the support structure manufactured in our shop. To test the system and adjust the lenses, we are using a helium beam from the accelerator on a thin aluminum foil to produce an energy and energy spread that match those calculated for the polonium source. The end station for our original microbeam was moved to the floor above because additional room for the lens structure was required between the table and the bending magnet. The first lens was adjusted to provide a good line image on a CCD mounted at the focal point of the lens. By adjusting the second lens, the beam has been focused to a spot $30\ \mu\text{m}$ in diameter using the compound lens system. Further adjustments of the lenses are expected to result in a beam spot $10\ \mu\text{m}$ in diameter.

A glove box has been purchased in which to plate the polonium on the wire to make the alpha source. This procedure is expected to be quite simple and exhaust all the polonium from the solution. A thin layer of gold will be plated over the source to contain the polonium. We are awaiting an amendment to our radioactive materials license so we can receive a small quantity of polonium as a test of the procedure.

Focused x-ray microbeam

We have investigated expanding the microbeam repertoire to include soft x-rays ($\text{Al } k_{\alpha}$, $1.49\ \text{keV}$). Microbeam studies with focused high-energy x-rays or gamma-rays are not feasible due to Compton scattering effects, so we are limited to x-ray energies where the predominant mode of interaction is photo-electron absorption. A proton beam will be focused onto an aluminum foil using the compound electrostatic lens. The characteristic x-rays produced in the foil then will be focused to a diameter of $1\ \mu\text{m}$ using a zone plate with a focal length of $12.7\ \text{mm}$. Calculations performed indicate that a $1\ \text{nA}$ proton beam should produce a dose rate of



Fig. 2 The original microbeam irradiation station moved to the floor above the original microbeam room (normally storage) for use in testing the stand alone microbeam system. One of the permanent magnet quadrupole triplets is inside the white enclosure (to keep it clean) in the middle of the table on the left.

$0.1\ \text{Gy/sec}$ of x-rays, adequate for the biological studies envisioned. An alternative system is being investigated in which a capillary tube with an inside diameter of a few microns would be used instead of a zone plate to collimate or focus the x-rays. The end of the microbeam line will be modified so that the target and focusing system can be rotated into or out of the beam path to change irradiation modalities quickly and without interrupting the vacuum system.

Precision z-motion stage

The high-precision stage from Mad City Labs in Wisconsin that also has a vertical motion is in routine use in the Microbeam II irradiation station. This stage has a range of motion of $200\ \mu\text{m}$ in the x and y directions and $100\ \mu\text{m}$ in the z direction, with nanometer positioning. Because of its limited range of motion in the horizontal plane, it has been mounted within a coarser stage in order to be able to access the entire area on which cells are plated. The vertical motion is required for the imaging techniques described below. The stage is also used to raise and lower the sample over the exit window during movement to minimize the separation from the window and thereby reduce beam spread due to scattering in the window.

Laser ion source

Development of the laser ion source continues to progress. The mounts for the mirrors and lenses to direct and focus the laser beam on the target have been constructed and installed and testing of the system has begun. The motor system advances the target surface along a spiral with each laser pulse in order to obtain a fresh surface and maintain yield. Methods are being examined to protect the focusing lens from material ejected by the target and to maintain the laser focus to prevent damage to the target.

The terminal of the new Singletron has been designed to accommodate the ion source without any modification to our present design. We have decided not to install the source in

the Van de Graaff, which could take up to a month for modifications to the terminal and testing, because the accelerator will be decommissioned at the end of April.

Secondary emission ion microscope

As we improve the spatial characteristics of the microbeam system, it becomes increasingly important to be able to assess the beam quality in order to adjust the system to its optimum capabilities. A secondary electron ion microscope (SEIM) has been designed and is currently being constructed. This device will enable us to measure the beam profile and position in real time with sub-micron resolution and sensitivity to single ions (1–5 MeV protons, as well as heavier ions). The SEIM design was inspired by the technique of photoelectron microscopy (PEM) and we gratefully acknowledge the advice of a world expert in PEM, Dr. Gertrude Rempfer, in finalizing our design. The SEIM is based on secondary electron emission (SEE) by a film on which the ions in the beam are incident. The ejected electrons are focused to form a magnified image on an image-intensified CCD. In order to overcome the chromatic and spherical aberrations inherent in the electrostatic lens and provide a more compact instrument, the electrons are bent by a 45° angle, reflected by an electrostatic mirror and bent by an additional 45° before reaching the detector. This “folded” design of the SEIM is a novel one, developed at RARAF. Calculations indicate a magnification of ~500 can be achieved, yielding a resolution of 0.1–0.2 μm .

We have built an “unfolded” SEIM, consisting of the electrostatic lens and the electron detector but without the magnet and mirror, in order to test the lens properties. For this version, simulations have shown that both the resolution and magnification are 10–20 times inferior to the folded SEIM. For testing and calibration purposes the SEE foil was replaced with a quartz window on which a micron scale pattern of aluminum was evaporated. The pattern was illuminated with low intensity UV light and the resulting photoelectrons were imaged, similar to a photoelectron microscope. In a sample image based on ~200,000 electrons the width of the spot edge allows us to estimate the SEIM resolution at 4.3 μm RMS, in good agreement with the prediction of 4–5 μm made by simulations. The predicted magnification (16x) is also in good agreement with the measured value of 20x.

The SAM would also be useful for groups that desire to perform microbeam experiments at their home institutions but lack an appropriate accelerator. It is estimated that a complete SAM system, including the microscope, could be built for ~\$100k.

Non-scattering particle detector

To irradiate thick samples, such as model tissue systems or oocytes, or to use particles with very short ranges, such as the heavy ions from the laser ion source, a completely non-scattering upstream particle detector is necessary. A novel particle detector has been designed on the basis of a long series of inductive cells coupled together into a delay line. The Lumped Delay Line Detector (LD²) will consist of 300 silver cylinders 3 mm long with a 2.2 mm inside diameter

connected by inductors and capacitively coupled to ground. The cylinders are glued to a semi-cylindrical tube of dielectric material 1 m long for mechanical support. The dielectric has a semi-cylindrical metal tube around it that can be rotated about its axis to adjust the capacitance. If the individual segment delays are set (by adjustment of the capacitance) such that the propagation velocity of the pulse equals the projectile velocity, the pulses induced in all segments will add coherently, giving a fast electron pulse at one end of the delay line that is 150 times larger than the charge induced on a single cylinder. This easily detectable charge of at least 150 electrons will be amplified to provide the detection pulse for the particle counter. The surface-mount inductors have been purchased. The silver cylinders originally purchased proved to be too eccentric and badly finished. Silver tubing has been purchased from which our shop will machine the cylinders. The rest of the detector parts have been designed and await machining. Testing of the detector will probably not begin until we have the new accelerator operational. It is anticipated that this detector will become the standard detector for all the irradiations on the new microbeam facility.

Advanced imaging systems

Development continued on new imaging techniques to view cells without using stain and to obtain three-dimensional images of unstained cells. Two different techniques are being investigated: phase-shifted interference microscopy and quantitative non-interference phase microscopy (QPm).

In phase-shifted interferometry images are obtained with an immersion Mirau interferometric objective in a sequence of three sub-wavelength path differences (phase shifts) between the sample and the lens. For this technique, it is important that the substrate for the cells be optically flat. The combined images can be used to produce a topographic image by solving for the phase shifts at each point. The essence of the algorithm for determining these phase shifts is to solve for three variables with an over-determined system of four equations. Results so far are encouraging. It has not yet been determined whether the cells will have to be on a reflective surface. The Mirau lens has been purchased and the immersion system has been designed, with assistance from Chun-Che Peng, one of the high school students.

The other method being investigated is a relatively new technique that can generate phase images and phase-amplitude images using a standard microscope. To obtain a quantitative phase image, an in-focus image and very slightly positively and negatively defocused images are collected. The resulting data can be used to yield the phase distribution by Fourier-transform methods. Test images sent to the software manufacturer yielded surprisingly good resultant images. We are evaluating a trial copy of the Fourier transform-based software for generating phase images or phase-amplitude images from the three microscope images.

Both of these techniques require rapid automated motion in the X-Y plane for locating the cells as well as in Z for changing the focal plane. In the case of immersion-based Mirau interferometry, the precision must be on the order of

tens of nanometers. The Mad City stage will be able to provide the vertical motion required by both these methods to obtain the necessary images at different distances between the sample and the lens.

A method of identifying the stage of the cell cycle using the microbeam image analysis system is being investigated. The Hoechst 33342 dye used to stain cell nuclei for identification in the microbeam irradiation system binds to the DNA in the nucleus. Cells in G2 have twice the DNA of cells in G0 or G1, with cells in S phase increasing from the level in G1 to that in G2. Consequently, it seems reasonable to believe that the amount of stain in a nucleus could be used to indicate which of these phases a cell is in. Initial measurements using cells synchronized in G1 by serum starvation have proven inconclusive. Additional measurements are continuing.

New Accelerator

The specifications for the Singletron from HVE in general exceed those for the Van de Graaff it is replacing. The maximum terminal voltage is 5 MV with 100 V or less ripple at 3 MV. The maximum voltage ever attained by the Van de Graaff was 4.4 MV and the ripple was never less than 1-2 kV. The maximum beam currents are 200 μ A of protons, 100 μ A of deuterons and 1 μ A of helium ions, similar to that of the Van de Graaff.

The Singletron is scheduled to be shipped by boat from the Netherlands about May 20 of this year and should arrive in port 1-2 weeks later. The Singletron will then be carried by truck to RARAF where it will be lifted by crane, placed on its rails and rolled into place. The Van de Graaff, of course, will have to be removed before then.

We will begin the process of disconnecting the Van de Graaff wiring and plumbing on May 2. All the old control wires and the racks that supply power to the accelerator will be removed. At the console, all the voltage regulation electronics and controls for the ion source and charging system also will be removed. The Singletron will be controlled by a computer at the console through a fiber-optic link to the accelerator rack. The accelerator vacuum system will be disconnected from the rest of the beam line and the interior of the Van de Graaff dismantled. The accelerator pressure vessel, the interior components and especially the base plate will be assayed to determine whether the pieces can be disposed of as regular scrap or will have to be handled as radioactive material. The interior of the acceleration tube will be tested for tritium contamination that may have occurred from years of using tritium targets to make neutrons, and decontaminated before disposal, if necessary.

Although the Van de Graaff was originally put in place using the overhead crane in the building, removal by the same method is no longer practical because of the shield blocks over the area and the labs that have been built on them, particularly the Microbeam II lab. Therefore, in order to remove the baseplate and pressure vessel, the rear wall of the building extension will be cut open and the accelerator pulled out onto a temporary platform where it will be lifted by crane onto a truck. Rails for the Singletron will be put in place on this platform temporarily so that the new accelera-

tor can be rolled in through the same opening. We anticipate the entire process of removing the Van de Graaff and putting the Singletron into place will take about one month.

After the building has been restored and the electric and fiber-optic cables are installed, a representative from HVE will supervise the assembly of the Singletron by the RARAF staff. Once the accelerator is assembled, performance tests will be made to certify that the accelerator meets (or exceeds) the specifications HVE stated in their bid. HVE estimates that this process will take 4-5 months, so that there will be a 5-6 month period when no accelerator will be available.

Accelerator Utilization and Operation

Accelerator usage is summarized in Table II. The accelerator now is started at 7:30 AM on most days and run into the evening on many nights for experiments, development and repair. In addition, Dr. Aprile's Astrophysics group (Exp. 123) has run continuously over a few weekends. This has resulted in a total use (117%, including repairs) that considerably exceeds the nominal accelerator availability of one 8-hour shift per weekday and is the highest we have had at Nevis Labs.

Use of the accelerator for radiobiology and associated dosimetry increased almost 50% over 2002-2003 and was about the same as the average for 1999 to 2003. About half the accelerator use for all experiments was for microbeam irradiations. Because of the relatively low number of cells that can be irradiated in a day, microbeam experiments usually require considerably more beam time than broad beam irradiations to obtain sufficient biological material, especially for low probability events such as transformation and mutation, and therefore normally constitute a large fraction of the experimental use.

Radiological physics utilization of the accelerator increased again this past year, primarily due to the calibration of the xenon detector (Exp. 123) that comprised about 18% of all the time used for experiments. On two weekends, this experiment ran continuously for 2½ days. As usual, there were no chemistry experiments this reporting period.

Use of the accelerator for online development declined about 15% over last year but still comprised over 40% of all available time. For several months, many more than the usual number of extra shifts was worked in the evening, on weekends and holidays.

Table II.
Accelerator Use, Nov. 2003-Oct. 2004
Percent Usage of Available Days

Radiobiology and associated dosimetry	37
Radiological physics and chemistry	14
On-line facility development and testing	42
Off-line facility development	17
Safety system	2.5
Accelerator-related repairs/maintenance	18
Other repairs and maintenance	1

Accelerator maintenance and repair time increased by 50% over last year, returning to the level of 2001–2002, and was also about 50% higher than the long-term average due to continued problems in the power supply in the terminal used to spray negative charge on the charging belt. Despite several modifications to the supply to reduce sparking, one of two strings of high voltage diodes in the supply would short out. We believe we now have located the cause of this problem and have repaired the power supply. The vacuum leak in one of the sections of the acceleration tube is a problem that has troubled us for several years, but at the moment is only an annoyance since a procedure has been developed to reseal the leak each time we open the accelerator for repair. No replacement of the section is planned because the accelerator will be dismantled in about 2 months to make room for the new one. No major repairs or modifications to the accelerator were performed. Once the new accelerator is installed, we anticipate much less accelerator maintenance, not only because the Singletron will be new, but also because it will be charged electronically (similar to a Cockroft-Walton) and will have few moving parts (no belt or chains). It has an RF ion source that also should require less maintenance than the Duoplasmatron source we are presently using. During the 5–6 months for the removal of the Van de Graaff and installation of the Singletron there will be no “on-line” development or accelerator-based experiments. All biology will be performed using the stand-alone microbeam. However, considerable development will continue since much of it is concerned with optical or other imaging issues and these don’t require an accelerator.

Training

This year we have had several students train at RARAF. During the summer of 2004, five students from Stuyvesant High School in Manhattan (Lusana Ahsan, Ross Kelly, Perry Leung, Deep Parikh, and Chun-Che Peng) spent at least two half days each week for 6 weeks working on projects in biology or physics that they selected. At the end of their projects, the students gave very professional presentations of their work. Their knowledge and commitment to their projects was impressive. This summer program for high school students now will be offered every year.

Ravash Eliassi, an undergraduate student from UCLA, spent ten weeks during the summer measuring the yields and neutron spectra produced by protons on a very thin beryllium target (Exp. 82). This type of target might be used to produce neutrons for the detection of explosives by resonant neutron scattering.

David Ross, an undergraduate student from the University of North Texas spent 4 weeks starting in December 2004 studying whether the phase of the cell cycle could be determined by the microbeam image analysis system using quantitative analysis of the Hoechst stain.

Personnel

The Director of RARAF is Dr. David Brenner. The Van de Graaff accelerator facility is operated by Mr. Stephen Marino and Dr. Gerhard Randers-Pehrson. Our ranks have now swelled to a total of seven physicists, an increase of

two.

Dr. Alan Bigelow, now an Associate Research Scientist, is continuing the development of the laser ion source and an optical system for 3-dimensional viewing of cells.

Dr. Guy Garty, a Staff Associate, is working on the development of a stand alone microbeam, the secondary emission ion microscope (SEIM) and an inductive detector (LD²) for single ions.

Mr. Greg Ross is a Programmer/Analyst, assisting with various programming tasks and working on the development of a stand alone microbeam and new methods of imaging cells.

Dr. Giuseppe Schettino, a Post-Doctoral Fellow, arrived in November from the Gray Lab in England. He will work primarily on the development of the x-ray microbeam.

Dr. Furu Zhan, a Post-Doctoral Fellow, returned to China in May, 2004.

Biologists from the Center for Radiological Research are stationed at the facility in order to perform experiments:

- Dr. Charles Geard, the Associate Director of the CRR, continues to spend most of each working day at RARAF. In addition to his own research, he collaborates with some of the outside users on experiments using the single-particle microbeam facility.
- Dr. Brian Ponnaiya is an Associate Research Scientist performing experiments using the track segment and microbeam irradiation facilities.
- Ms. Gloria Jenkins, a Biology Technician, performs experiments on the microbeam facility for Dr. Geard.
- Dr. Stephen Mitchell, a Post-Doctoral Fellow, continues to perform research involving neoplastic transformation of cells.

Recent Publications of Work Performed at Raraf (2003–2004)

1. Amundson SA, Do KT, Vinikoor L, Koch-Paiz CA, Bittner ML, Trent JM, Meltzer P and Fornace AJ Jr. Stress-specific signatures: Expression profiling of p53 wild-type and null human cells. *Oncogene* Apr 11, 2005 [Epub ahead of print].
2. Balajee AS, Geard CR. Replication protein A and gamma-H2AX foci assembly is triggered by cellular response to DNA double-strand breaks. *Exp Cell Res* **300**:320-34, 2004.
3. Balajee AS, Ponnaiya B, Baskar R and Geard CR. Induction of replication protein a in bystander cells. *Radiat Res* **162**:677-86, 2004.
4. Balajee AS and Geard CR. Replication protein A relocates into distinct nuclear foci and co-localizes with γ -H2AX in response to DNA damaging agents. (Submitted to *Radiat Res*, 2004.)
5. Bigelow AW, Randers-Pehrson G, Kelly RP and Brenner DJ. Laser Ion Source for Columbia University’s Microbeam. *Nucl Instr Meth B* (in press 2005).
6. Bigelow AW, Ross GJ, Randers-Pehrson G and Brenner DJ. The Columbia University Microbeam II endstation for cell imaging and irradiation. *Nucl Instr Meth B* (in press 2005).
7. Garty G, Randers-Pehrson G and Brenner DJ. Develop-

- ment of a secondary-electron ion-microscope for microbeam diagnostics. *Nucl Instrum Meth B* (in press 2005).
8. Garty G, Ross GJ, Bigelow A, Randers-Pehrson G and Brenner DJ. A microbeam irradiator without an accelerator. *Nucl Instrum Meth B* (in press 2005).
 9. Geard CR and Ponnaiya B. Chromosomal changes and cell cycle checkpoints in Mammalian cells. *Methods Mol Biol* **241**:315-28, 2004.
 10. Hei TK, Persaud R, Zhou H and Suzuki M. Genotoxicity in the eyes of bystander cells. *Mutat Res* **568**:111-20, 2004.
 11. Ponnaiya B, Jenkins-Baker G, Bigelow A, Marino S and Geard CR. Investigation of a radiation-induced bystander effect in human fibroblasts using co-culturing protocols. (Submitted to *Int J Radiat Biol*, 2004.)
 12. Ponnaiya B, Jenkins-Baker G, Bigelow A, Marino S and Geard CR. Investigation of the role of cell type specificity in the induction of a bystander effect. (Submitted to *Int J Radiat Biol*, 2004).
 13. Ponnaiya B, Jenkins-Baker G, Bigelow A, Marino S and Geard CR. Detection of chromosomal instability in α -irradiated and bystander human fibroblasts. *Mutat Res* **568**:41-8, 2004.
 14. Ponnaiya G, Jenkins-Baker G, Brenner DJ, Hall EJ, Randers-Pherson G and Geard CR. Biological responses in known bystander cells, relative to known microbeam irradiated cells. *Radiat Res* **162**:426-32, 2004.
 15. Ross GJ, Garty G, Randers-Pehrson G and Brenner DJ. A single-particle/single-cell microbeam based on an isotopic alpha source. *Nucl Instrum Meth B* (in press 2005).
 16. Suzuki M, Zhou H, Geard CR and Hei TK. Effect of medium on chromatin damage in bystander mammalian cells. *Radiat Res* **162**:264-269, 2004.
 17. Suzuki M, Zhou H, Hei TK, Tsuruoka C and Fujitaka K. Induction of a bystander chromosomal damage of He-ion microbeams in mammalian cells. *Biol Sci Space* **17**:251-2, 2003. ■



The new RARAF stand-alone microbeam: a) Diagram of the stand-alone microbeam's principle elements. A small, high specific-activity α -emitter is used as a source. A compound magnetic lens, consisting of 24 permanent magnets arranged in two quadrupole triplets, focuses the emitted α -particles. The first triplet is placed 2 m above the source, with a second identical triplet placed 2 m above the focal plane of the first. The cells to be irradiated are placed at the image plane on a voice coil stage. The endstation consists of the voice coil stage and a microscope with a particle detector mounted on the objective lens. b) The microbeam endstation and immediately below it the upper magnetic quadrupole triplet. c) The source holder (near floor) and the lower quadrupole triplet. d) A system for electroplating polonium onto the end of a wire, to create the 1-mm diameter, α -particle source.